Learning Low-dimensional Multi-domain Knowledge Graph Embedding via Dual Archimedean Spirals

Jiang Li[1,2] , **Xiangdong Su**[1,2] * , **Fujun Zhang**[1,2], **Guanglai Gao**[1,2]
[1] College of Computer Science, Inner Mongolia University, Hohhot, China
[2] National & Local Joint Engineering Research Center of Intelligent Information Processing Technology for Mongolian, Hohhot, China
lijiangimu@gmail.com, {cssxd,csggl}@imu.edu.cn, 32209093@mail.imu.edu.cn

Abstract

Knowledge graph embedding (KGE) is extensively employed for link prediction by representing entities and relations as low-dimensional vectors. In real-world scenarios, knowledge graphs (KGs) usually encompass diverse domains, which poses challenges to KG representations. However, existing KGE methods rarely make domain constraints on the embedding distribution of multi-domain KGs, leading to the embedding overlapping of different domains and performance degradation of link prediction. To address this challenge, we propose **Du**al **A**rchimedean **S**piral Knowledge Graph **E**mbedding (DuASE), a low-dimensional KGE model for multi-domain KGs. DuASE is inspired by our discovery that relation types can distinguish entities from different domains. Specifically, DuASE encodes entities with the same relation on the same Archimedean spiral, allowing it to differentiate the entities from different domains. To avoid embedding overlapping across domains, DuASE further makes the head and the tail spirals in the same triplet cluster to their respective domain space by a regularization function. Thus, DuASE can better capture the domain information and the dependencies between entities when modeling the multi-domain KGs, leading to improved KG representations. We validate the effectiveness of DuASE on the novel multi-domain dataset (n-MDKG) introduced in this study and three other benchmark datasets[1].

1 Introduction

Knowledge graphs (KGs) represent networks of real-world entities and describe the associations between them, which play a crucial role in various tasks, including large language models (Zhao et al., 2023; Hu et al., 2023; Pan et al., 2024), information retrieval (Gaur et al., 2022) and question answering (Saxena et al., 2022). Nonetheless, the incompleteness of KGs will lead to unfavorable outcomes in related tasks. Therefore, researchers propose many knowledge graph embedding (KGE) approaches (Bordes et al., 2013; Lin et al., 2015) to predict the missing links based on the known triplets. Since high-dimensional KGE methods require large memory and high computation costs (Zhu et al., 2022), the low-dimensional KGE methods have gained popularity (Balazevic et al., 2019a; Chami et al., 2020; Nayyeri et al., 2023).

However, most existing KGE methods, including low-dimension methods, ignore the multi-domain characteristics of KGs, and mining multi-domain information within KGs is essential for enhancing link prediction performance. In the context of KG, the term "domain" is used to describe a specific subject area or category of knowledge that the KG encompasses or represents.

In reality, most KGs span a variety of domains, including sports, medicine, law, history, etc. The ignorance of making domain distinctions in KGE leads to the problem of embedding overlapping across different domains, consequently impairing the effectiveness of link prediction. As shown in Figure 1, there are overlaps among the embeddings learned by the ComplEx, RotatE, and RotH on the 6-MDKG dataset with six domains. More details about embedding overlapping cross domains are computed via the Jaccard index and discussed in **Appendix A**. In fact, if the KGE model takes into account the distinction between domains, it can reduce the errors in the link prediction section. This is because there are significant differences in the types of relationships between entities in different domains.

To effectively model multi-domain KGs, this paper imposes domain constraints in KGE and proposes a low-dimensional KGE model DuASE, which avoids the embedding overlapping and im-

* Corresponding Author
[1] Code and datasets are available at https://github.com/dellixx/DuASE

Findings of the Association for Computational Linguistics: ACL 2024, pages 1982–1994

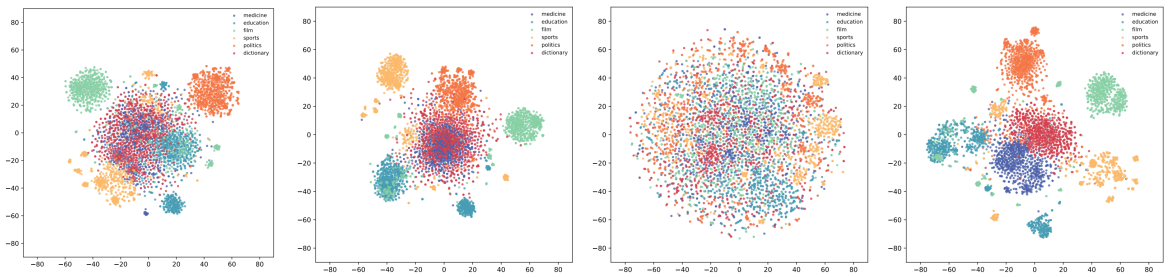

(a) ComplEx (b) RotatE (c) RotH (d) DuASE (ours)

Figure 1: Visualizations of entities on six different domains. Different colors indicate different domains.

proves the performance of link prediction. Our motivation is based on the following two aspects. **First, it is reasonable to distinguish different domains via the relations in the KG triplets.** In KGs, the differences among domains are mainly in entity types and relation types. Since entity type information is not available in most KGs, we mainly rely on relation types in knowledge triplets to accomplish domain knowledge differentiation. We list some domains and their relations: (a) Medical Domain: Treatment, Diagnosis, Prescription, etc. (b) Film Domain: Directing, Cinematography, Directed, etc. (c) Literature Domain: Publication, Critique, Adaptation, etc. **Second, spiral provides the possibility of modeling KG domains and avoiding embedding overlapping by mapping *entities* onto *relation* spirals.** The term Archimedean spiral is defined as: $\varphi = a + b \cdot \theta$. Different spirals can model various relations for domain distinguishing through parameter b, and different rotation angles (parameter θ) of the same spiral can model different entities.

Specifically, DuASE maps the entities in knowledge triplets onto the relation Archimedean spiral. DuASE further enforces the dual spirals of the head and the tail entities in the same triplet to be as close as possible by a regularization function. This clusters the learned embedding into their respective domain space and avoids the embedding overlapping across different domains. Thus, DuASE can better capture the domain information and the dependencies between entities when modeling the multi-domain KGs, leading to improved KG representations. Figure 1 shows that the proposed DuASE can effectively model domain distinction. We validate the effectiveness of DuASE on our proposed multi-domain dataset (n-MDKG) and three other benchmark datasets.

Furthermore, benefiting from the proposed dual Archimedean spirals, DuASE can capture important relation patterns (symmetry, antisymmetry, inversion and composition) in low-dimensional space. We provide formal proofs of such ability of our model in **Appendix B**. It further reinforces the reliability and robustness of our model in capturing meaningful patterns and associations among entities.

Our contributions are summarized as follows:

- The proposed DuASE can effectively model the multi-domain KGs by mapping entities with the same relation onto the same Archimedean spiral. To our knowledge, this work is the first to investigate domain distinction in low-dimensional KGE.
- We propose a novel regularizer to promote the proximity of the dual spirals of the head and the tail entities in the same triplet. Thus, DuASE can better model the domain differences and alleviate the embedding overlapping problem in KGE.
- To evaluate the effectiveness of the KGE methods on multi-domain KGs, we develop a novel multi-domain KGE dataset named n-MDKG, since most KGs involve multiple domains and the domain labels are not explicitly annotated.

2 Related Work

2.1 KGE Methods

The representations of distance-based models TransE (Bordes et al., 2013), which defines the relations r as translations from head entities h to tail entities t. The scoring function in TransE is denoted as the distance between $h + r$ and t with the l_1 or l_2 parametric constraints. After that, TransH (Wang et al., 2014), TransR (Lin et al., 2015) and TransD (Ji et al., 2015) enhance KGE representations through diverse projection strategies. In addition, RESCAL (Nickel et al., 2011)

and DistMult (Yang et al., 2015) adopt scoring functions based on similarities between head, relation and tail embeddings. ComplEx (Trouillon et al., 2016) and RotatE (Sun et al., 2019) extend these methods by operating in the complex space, providing enhanced expressiveness for handling asymmetric relations. More recently, TuckER (Balazevic et al., 2019b) and AutoSF (Zhang et al., 2020) introduce increased flexibility in modeling similarities. Since high dimensionality KGE increases the computational complexity and memory requirements, our work focuses on the low-dimensional KGE methods in multi-domain KGs.

2.2 Low-dimensional KGE Methods

In recent times, there has been a growing interest in developing low-dimensional Knowledge Graph Embedding (KGE) methods. MuRP (Balazevic et al., 2019a) adopts the hyperbolic space for entity and relation embeddings, effectively capturing hierarchical structures within KGs. Furthermore, RotH, RefH and AttH (Chami et al., 2020) enhance hyperbolic KGE by incorporating hyperbolic isometries to model symmetry and antisymmetry patterns in KGs. However, hyperbolic geometry-based calculations involve complex Möbius matrix-vector multiplication and Möbius addition operations. To address this, the Rot2L (Wang et al., 2021a) model simplifies hyperbolic operations.

In addition, MulDE (Wang et al., 2021b) and DualDE (Zhu et al., 2022) use knowledge distillation to learn low-dimensional KG embeddings. However, they require a long training time to learn low-dimensional features. Itô̂E (Nayyeri et al., 2023) models relations in the KG as stochastic processes, which introduces complexity to the training process. Although the above methods employ distinct strategies to enhance low-dimensional KGE representations, these approaches infrequently delve into the multi-domain information in multi-domain KGs.

Unlike existing KGE methods, we are the first to explore the low-dimensional multi-domain KGE approach. The proposed DuASE encodes entities with the same relation onto the same relation spiral space. Moreover, it demonstrates the ability to capture important relation patterns (symmetry and antisymmetry, inversion and composition) simultaneously in low-dimension space. Notably, DuASE operates in the complex space, which is less intricate compared to hyperbolic space. Besides, DuASE employs linear operations for efficient processing.

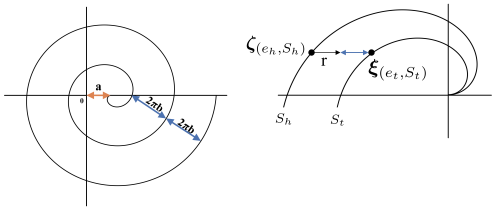

(a) (b)

Figure 2: (a) shows an illustration of an Archimedean spiral. (b) shows an illustration of our model.

3 Background and Notation

3.1 Archimedean Spiral

In mathematics, the Archimedean spiral, also known as the arithmetic spiral, is a curve named after the ancient Greek mathematician Archimedes, who lived in the 3rd century BC. Figure 2(a) illustrates the locus representing the positions of a point moving away from a fixed point at a constant speed along a line that rotates with a constant angular velocity. This spiral can be expressed in polar coordinates (φ, θ) using the equation:

$$\varphi = a + b \cdot \theta, \tag{1}$$

where a controls the distance from the starting point of the spiral to the origin, b controls the distance between loops, and θ represents the angle of rotation of the spiral. The distance between consecutive loops is $2\pi b$. In addition, we also consider the Logarithmic spiral, represented by their respective formulas $\varphi = ae^{b\theta}$. Based on an initial verification experiment, we have concluded that both spirals can be utilized to model multi-domain KGs. However, due to their complexities, we employ the simpler Archimedean spiral in the proposed DuASE.

3.2 Knowledge Graph Embedding

A knowledge graph is typically denoted as $\mathcal{G} = (\mathcal{E}, \mathcal{R}, \mathcal{T})$, where $\mathcal{E}$, $\mathcal{R}$ and $\mathcal{T}$ represent the sets of entities, relations and triplets (h, r, t), respectively. The KGE task computes the score function $f_r(h, t)$ and anticipates that the scores of correct triplets will be higher than those of invalid triplets. Specifically, the KGE task aims to accurately learn embedded representations of entities, relations to facilitate predictions of missing entities in KGs. It

involves predicting the tail entity t given a tuple $(h, r, ?)$, or conversely, predicting the head entity h for a tuple $(?, r, t)$.

4 Methodology

4.1 The Proposed DuASE

The proposed **Du**al **A**rchimedean **S**piral Knowledge Graph **E**mbedding (DuASE) is inspired by our discovery that the domains can be distinguished by the relations in the knowledge triples. For example, the triplets from the three different domains (edu., film, pol.) are as follows: (Stanford University, *school_type*, Private University), (Spider Man3, *film_by*, Stan Lee), (china, *make a visit*, bahrain) and (barack obama, *consult*, poland). Based on such fact, we map the entities with the same relation on the same spiral to distinguish entities from different domains.

The term spiral is usually used for the more general group of spirals: $\varphi = a + b \cdot \theta^{\frac{1}{c}}$. The Archimedean spiral occurs when $c = 1$. Other spirals falling into this group include the hyperbolic spiral ($c = -1$), Fermat's spiral ($c = 2$), and the lituus ($c = -2$). Given their complexities, we chose the simpler Archimedean spiral ($c = 1$) in the proposed DuASE.

Specifically, DuASE encodes the entities on the relation Archimedean spiral, in which all the entities with the same relation are on the same spirals. We defined two spiral lines (S_h and S_t), and mapped the head entity h and the tail entity t onto their respective relation spirals, S_h and S_t, as shown in Figure 2(b). S_h denotes the spiral corresponding to the head entity h and S_t denotes the spiral corresponding to the tail entity t. The dual spirals (S_h and S_t) provide the ability to constrain the domain space in our model. DuASE regards each entity as different the angle of rotation θ in Eq. 1, and regards S_h and S_t as distance control parameter b in Eq. 1. Thus, the range of embedding values for each entity is $\boldsymbol{e}_h, \boldsymbol{e}_t \in (0, 2\pi)$. In addition, to prevent crossover between domains space, we set the starting point of all spirals to the origin. That is, we set $a = 0$ for DuASE in Eq. 1. Formally, the head entity and tail entity when mapped onto the S_h and S_t respectively are represented as:

$$\boldsymbol{\zeta}_{(e_h,S_h)} = \boldsymbol{e}_h \circ S_h, \quad \boldsymbol{\xi}_{(e_t,S_t)} = \boldsymbol{e}_t \circ S_t. \tag{2}$$

Since many previous works (Trouillon et al., 2016; Sun et al., 2019) have demonstrated that encoding knowledge graphs in complex space can better capture potential links between entities, we also model KGs in the complex space, i.e., $\boldsymbol{e}_h, \boldsymbol{e}_r, \boldsymbol{e}_t, \in \mathbb{C}^d$. For each triplet (h, r, t), we define the relation as translation from $\boldsymbol{\zeta}_{(e_h,S_h)}$ to $\boldsymbol{\xi}_{(e_t,S_t)}$. To remove translation freedom, we also add embedding constraints similar to previous distance-based KGE models (Bordes et al., 2013; Chao et al., 2021). We aim for the dual spirals (S_h and S_t) to better distinguish domain knowledge and we apply an L_2-norm for the relation embeddings $\boldsymbol{e}_r$. The score function of DuASE is denoted as:

$$f_r(\boldsymbol{e}_h, \boldsymbol{e}_t) = - \parallel \boldsymbol{\zeta}_{(e_h,S_h)} + \boldsymbol{e}_r - \boldsymbol{\xi}_{(e_t,S_t)} \parallel . \tag{3}$$

The score function is used in the loss function to optimize the graph embeddings. In addition, we discuss the relation between DuASE and other models in **Appendix C**. In addition, Li et al. (2023) employs single Archimedean Spiral to model timestamps in temporal KG and maps relations onto timestamp spirals. The relation is defined as the parametric angle (θ). On the contrary, This paper designs Dual Archimedean Spirals to learn the domain information of entities. The entity is defined as the parametric angle (θ).

4.2 Loss Function

To optimize our model, we employ the self-adversarial negative sampling loss for DuASE, which is defined as:

$$\begin{aligned} \mathcal{L}_\mu = &- \log \sigma(\gamma - f_r(\boldsymbol{e}_h, \boldsymbol{e}_t)) \\ &- \sum_{i=1}^{n} p(h'_i, r, t'_i) \log \sigma(f_r(\boldsymbol{e}'_h, \boldsymbol{e}'_t) - \gamma), \end{aligned} \tag{4}$$

where σ is the sigmoid function, and γ is a fixed margin.

In addition, to further optimize the entity representations and constrain domain information in different domain space, we propose a novel regularization function to facilitate the convergence of the head and the tail spirals (S_h and S_t) in the same triplet. This constraint process ensures that DuASE can better capture the domain information between the head and the tail entity. The regularization function is defined as:

$$\mathcal{L}_\varsigma = \frac{1}{N_\mathcal{R}} \sum_{i=1}^{N_\mathcal{R}} \|S_h - S_t\|_2^2, \tag{5}$$

where $N_{\mathcal{R}}$ is the number of relations. Hence, the total loss function of DuASE is defined as:

$$\mathcal{L} = \mathcal{L}_{\mu} + \lambda \mathcal{L}_{\varsigma}, \tag{6}$$

where λ denotes the regularization coefficient. This function aims to minimize the distance between S_h and S_t for entities belonging to the same triplet, thereby enhancing the model's ability to distinguish between different domains while maintaining coherence within the same domain.

5 Experiments

5.1 Multi-domain Datasets n-MDKG

Since most KGs involve multiple domains and the domain labels are not explicitly annotated, we develop a novel multi-domain KGE dataset named n-MDKG, including **3-MDKG**, **6-MDKG** and **9-MDKG**, to facilitate the evaluation of the KGE methods on multi-domain KGs. In this dataset, we explicitly defined the domains contained in the dataset, as well as the relation types within each domain, maintaining independence between domains as much as possible. This allows for the evaluation of KGE models' ability of domain distinguishing in the case of different numbers of domains. The key difference between our proposed dataset and existing KG datasets is that the latter do not have domain labels and domain numbers, making it impossible to evaluate models on domain-level modeling capabilities. Given that domain differences are mainly reflected in the types of relationships, we distinguished domains based on these relationships and extracted data from multiple domains on this basis, combining them to form the dataset in this paper. We allow users to flexibly share and adapt the dataset for their use. A summary of n-MDKG is presented in **Appendix D**.

5.2 Benchmark Datasets

In addition, to further validate the effectiveness of our model, we conduct additional experiments on three other KGE benchmark datasets including **WN18RR** (Dettmers et al., 2018), **FB15K-237** (Toutanova and Chen, 2015) and **YAGO3-10** (Suchanek et al., 2007). A summary of these datasets is presented in **Appendix E**.

5.3 Evaluation Protocol

Following the existing low-dimensional KGE methods, we employ four standard metrics to evaluate our model, including Mean Reciprocal Rank (MRR) and H@n. The quality of the ranking of each test triplet is evaluated by considering all possible substitutions of the head entity and tail entity, denoted as (h', r, t) and (h, r, t'), where h' and t' belong to the set of entities $\mathcal{E}$. H@k measures the percentage of correct entities among the top k predictions, and higher values of MRR and H@k indicate better performance. The evaluation H@k is conducted with cut-off values $k = 1, 3, 10$.

5.4 Experimental Setup

We conduct all experiments on a single NVIDIA Tesla V100 with 32GB memory. We utilize the Adam (Kingma and Ba, 2015) optimizer and performed grid search to find the optimal hyperparameters based on the performance on the validation set. We train our model with 5 different random seeds $(0, 1, 2, 3, 4)$ and we report the average and unbiased standard deviation on the test set. The experimental settings are: learning rate $\in [0.1, 0.01, 0.001, 0.0001]$, fixed margin γ: $2 \sim 30$, fixed embedding dimension: 32, batch size $\in [1024, 2048]$, negative sampling $\in [256, 512]$.

6 Results and Analysis

6.1 Results on Multi-domain KGE Datasets

To evaluate the effectiveness of our proposed method, we conduct experiments in the low dimensionality setting of $d = 32$ on three multi-domain KG datasets including 3-MDKG, 6-MDKG and 9-MDKG. We compare our approach against general KGE methods and low-dimensional KGE methods, as shown in Table 1. Moreover, these models offer interpretability for learning structured relation patterns in KGs, allowing for a better understanding of the underlying mechanisms behind their performance. Hence, we use these models as the main baselines. In this study, our work focuses on the low-dimensional KGE methods in multi-domain KGs.

The experimental results demonstrate the superiority of our approach. DuASE consistently outperforms all other techniques in MRR, H@1, H@3 and H@10 metrics, further confirming its efficacy in predicting missing links in multi-domain KGs. We also report the standard deviations for the performance of our model, indicating the stability and reliability of our results. Our proposed KGE method DuASE encodes entities with the same relations on the same relation spiral, allowing it to differentiate the entities embedding from

	3-MDKG				6-MDKG				9-MDKG			
Method	MRR	H@1	H@3	H@10	MRR	H@1	H@3	H@10	MRR	H@1	H@3	H@10
KGE Methods												
TransE	0.126	0.082	0.135	0.214	0.170	0.098	0.196	0.310	0.029	0.014	0.030	0.057
RotatE	0.202	0.120	0.225	0.369	0.230	0.172	0.255	0.338	0.212	0.161	0.233	0.309
ComplEx-N3	0.189	0.106	0.208	0.366	0.233	0.187	0.252	0.317	0.272	0.232	0.288	0.347
low-dimensional Methods												
MurE	0.213	0.151	0.240	0.340	0.175	0.121	0.138	0.277	0.071	0.042	0.074	0.126
RotE	0.266	0.184	0.290	0.433	0.169	0.120	0.179	0.260	0.157	0.109	0.164	0.249
AttE	0.218	0.152	0.248	0.348	0.168	0.120	0.177	0.259	0.075	0.043	0.082	0.138
RotH	0.279	0.194	0.315	0.441	0.268	0.227	0.283	0.348	0.300	0.263	0.319	0.372
AttH	0.263	0.189	0.301	0.436	0.261	0.210	0.276	0.339	0.297	0.247	0.301	0.365
Rot2L	0.272	0.192	0.314	0.444	0.270	0.219	0.281	0.343	0.305	0.251	0.319	0.371
DualDE	0.265	0.188	0.305	0.438	0.268	0.215	0.278	0.338	0.316	0.249	0.313	0.369
DuASE (ours)	**0.301** ± 0.0031	**0.211** ± 0.0025	**0.336** ± 0.0011	**0.475** ± 0.0038	**0.287** ± 0.0029	**0.236** ± 0.0014	**0.306** ± 0.0037	**0.382** ± 0.0018	**0.324** ± 0.0023	**0.278** ± 0.0044	**0.340** ± 0.0020	**0.407** ± 0.0022

Table 1: Link prediction results on 3-MDKG, 6-MDKG and 9-MDKG (low dimension $d = 32$).

different domains. As a result, DuASE gains significant improvements in KG representations in multi-domain KGs and achieves better link prediction performance.

Model	Training Time
TransE	1.00 x
RotatE	1.07 x
MurE	1.12 x
RotE	1.65 x
AttE	2.28 x
RotH	11.47 x
AttH	11.53 x
DuASE (ours)	1.08 x

Table 2: The training time comparison between DuASE and baselines on 6-MDKG.

In addition, Table 2 shows a comparative analysis of the training time between our model and the baselines. All models are trained on a single NVIDIA V100 GPU. We can observe that our model and RotatE require less training time compared with other models. The increased training time for the models ROTH and ATTH is attributed to the complex computations involved in modeling in the hyperbolic space. This further validates the lightweight of DuASE in modeling KGs in low-dimensional spaces. The saved training time, especially when compared with competitive hyperbolic space models, demonstrates the effectiveness and computational advantage of our KGE approach in low-dimensional space.

6.2 Results on Benchmark KGE Datasets

To further validate the generalization capability of our model, we conduct experiments with a low dimensionality setting of $d = 32$ on public benchmark datasets including WN18RR, FB15K-237 and YAGO3-10. The results are summarized in Table 3. We can observe that DuASE consistently outperforms all other methods in terms of MRR and H@n metrics on WN18RR and YAGO3-10. In addition, DuASE achieves competitive results in H@3 and H@10, and comparable results in MRR and H@1 on the FB15K-237 dataset. Upon our further analysis, we discover that these benchmark datasets contain multiple subdomains. DuASE improves the entity embedding representations by learning multiple subdomain knowledge, leading to the competitive results of our model on these datasets.

6.3 Effect on Alleviating Entity Embedding Overlapping

To analyze the effective of the proposed DuASE in modeling multi-domain KGs, we employ T-SNE (Van der Maaten and Hinton, 2008) to visualize the entity embeddings learned by different models from multi-domain on 9-MDKG. The results are shown in Figure 1. We observe that there are obvious overlapping of entity embeddings learned by the ComplEx and RotatE models. The RotH model displays a hierarchical structure from the inner to the outer layers, characteristic of its hyperbolic space modeling. However, it is less sensitive to the multi-domain patterns present in KGs. It is obvious that the existing KGE models that are difficult to effectively learn the domain information of enti-

	WN18RR				FB15K-237				YAGO3-10			
Method	MRR	H@1	H@3	H@10	MRR	H@1	H@3	H@10	MRR	H@1	H@3	H@10
KGE Methods												
TransE	0.150	0.009	0.251	0.387	0.270	0.177	0.303	0.457	0.324	0.221	0.374	0.524
ComplEx-N3	0.420	0.390	0.420	0.460	0.294	0.211	0.322	0.463	0.336	0.259	0.367	0.484
RotatE	0.387	0.330	0.417	0.491	0.290	0.208	0.316	0.458	0.419	0.321	0.475	0.607
low-dimensional Methods												
MuRE	0.458	0.421	0.471	0.525	0.313	0.226	0.340	0.489	0.283	0.187	0.317	0.478
MuRP	0.465	0.420	0.484	0.544	0.323	0.235	0.353	0.501	0.230	0.150	0.247	0.392
REFE	0.455	0.419	0.470	0.521	0.302	0.216	0.330	0.474	0.370	0.289	0.403	0.527
REFH	0.447	0.408	0.464	0.518	0.312	0.224	0.342	0.489	0.381	0.302	0.415	0.530
ROTE	0.463	0.426	0.477	0.529	0.307	0.220	0.337	0.482	0.381	0.295	0.417	0.548
ROTH	0.472	0.428	0.490	0.553	0.314	0.223	0.346	0.497	0.393	0.307	0.435	0.559
ATTE	0.456	0.419	0.471	0.526	0.311	0.223	0.339	0.488	0.374	0.290	0.410	0.537
ATTH	0.466	0.419	0.484	0.551	0.324	0.236	0.354	0.501	0.397	0.310	0.437	0.566
Rot2L$^{\diamondsuit}$	0.475	0.434	-	0.554	0.326	0.237	-	0.503	-	-	-	-
DualDE$^{\diamondsuit}$	0.468	0.419	0.486	0.560	0.306	0.216	0.338	0.489	-	-	-	-
ItδE$^{\diamondsuit}$	0.455	0.404	0.480	0.548	**0.330**	**0.242**	0.361	0.508	-	-	-	-
DuASE (ours)	**0.489** ±0.0011	**0.448** ±0.0016	**0.503** ±0.0022	**0.569** ±0.0041	0.329 ±0.0011	0.235 ±0.0019	**0.364** ±0.0014	**0.519** ±0.0005	**0.473** ±0.0032	**0.387** ±0.0050	**0.524** ±0.0022	**0.628** ±0.0017

Table 3: Link prediction results on WN18RR, FB15K-237 and YAGO3-10 (low dimension $d = 32$). The results of $\diamondsuit$ are taken from the original papers. Other results are taken from Chami et al. (2020). Dashes denote the results are not reported in the corresponding literature.

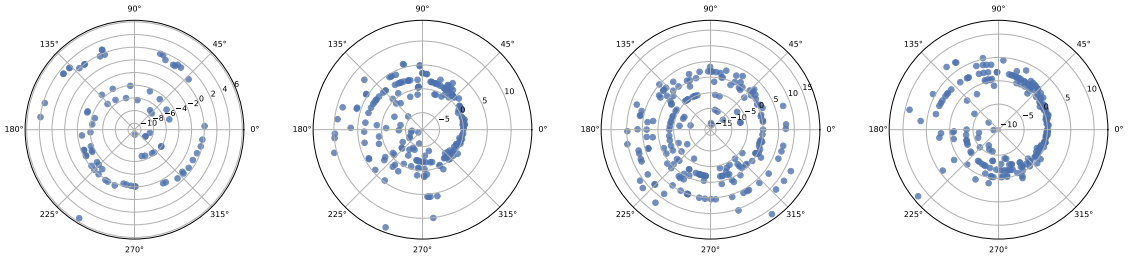

(a) *drug_protein* (b) *film_actor* (c) *educational_institution* (d) *hypernym*

Figure 3: Visualizations of the learned entity embeddings are mapped the corresponding relation domain.

ties. In contrast, our model exhibited remarkable capability in distinguishing entities from different domains. The differentiation in entity embeddings from diverse domains serves as evidence of the efficacy of our model in modeling multi-domain KGs.

In addition, we employ the Archimedean spiral to map entities into the polar coordinate system. Specifically, we map the learned entity embeddings to the corresponding relation spirals in the polar coordinate system. The results are shown in Figure 3 in Sec. 1. The mapping algorithm is based on the score function of DuASE. Figure 3 shows the entity embedding projection for four different relations from different domains. We can observe a spiral trend for entities on the same domain relation. These results indicate that DuASE can effectively learn the representations of entities through relation spirals and thus model the domains for the multi-domain KGs.

6.4 Effect of Regularizer Function

In this section, we study the effect of regularization on WN18RR and present the MRR metrics on the validation set in Figure 4. We plot a detailed comparison of our proposed regularizer to nuclear 3-Norm regularization (Lacroix et al., 2018). We note that the range of weight values corresponding to the peak values of different regular function waves is different. This is because the regularizer function constrained in different ways will lead to differences in regularization weights λ. The results show that our proposed dual spirals regularisation function for DuASE can better model multi-domain KG in low-dimensional space. Here, dual spirals regularizers drive the head spiral S_h and the tail

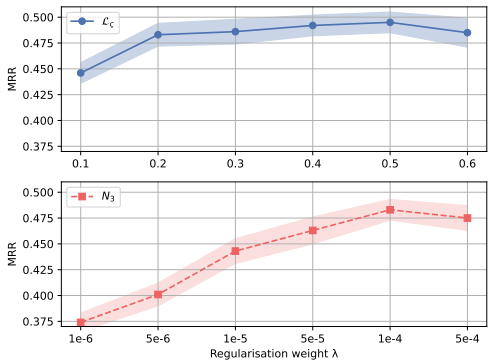

Figure 4: Link prediction results of DuASE trained with different regularizers on WN18RR dataset.

spiral S_t to converge to the same domain space. Thus, DuASE can better learn the domain information and the dependencies between entities when modeling the multi-domain KGs.

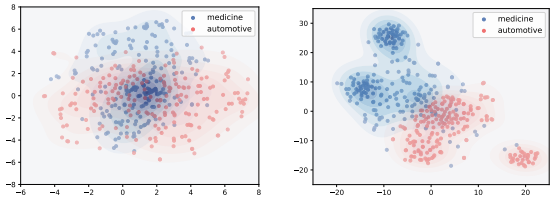

(a) (b)

Figure 5: Visualizations of the learned entity embeddings distribution on 9-MDKG. (a) without dual spirals regularizer. (b) with dual spirals regularizer.

In addition, we conduct experiments on 9-MDKG to verify the effectiveness of dual spirals regularizer function. We visualize the distribution of entities from two different domains (medicine and automotive), as shown in Figure 5. We can see that DuASE can better learn the domain information of entities by constraining the head and the tail spirals via dual spirals regularizer function. The results demonstrate that it is effective to cluster the entities into their respective domains and enhance the entity representations by learning domain information.

6.5 Further Visualisation Analyses

In Figure 6 (a), we visualize the entity embeddings learned by DuASE for a sub-tree of the organism entity on WN18RR. We can observe that our model can effectively learn semantic hierarchy information. DuASE can model hierarchical relation dependencies by mapping entities onto the corresponding

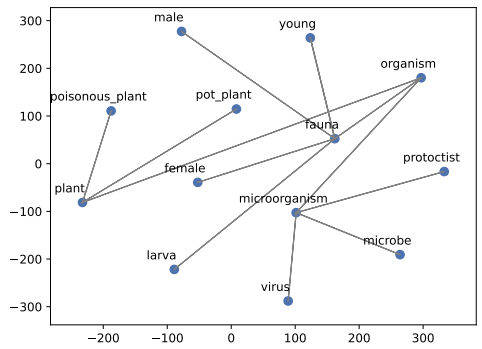

(a) A sub-tree of the organism entity.

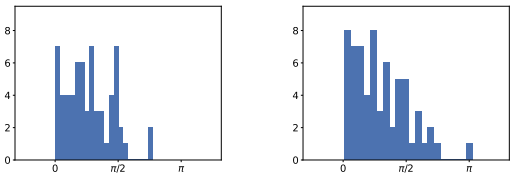

(b) *microorganism* (c) *organism*

Figure 6: (a) shows visualization of the learned entity embeddings on WN18RR dataset. (b) and (c) are distribution histograms of two entity embeddings.

relation spirals. As described in the methodology section, we treat entities as the angle of rotation of the spiral. Hence, $Emb(entity) \in (0, 2\pi)$. This capability empowers the model to distinguish between various entity representations on the same relation through angle rotation θ, enabling the effective modeling of hierarchical relation pattern. We also visualize the entity distribution histograms (*microorganism* $\subseteq$ *organism*) as shown in Figure 6 (b) and Figure 6 (c), respectively. We can observe that both organism and microorganism entities have different components between 0 and π, and these angle components allow for distinguishing entities in the same domain space.

7 Conclusion

Given the importance of mining domain information in multi-domain KGE and the fact that relations play an important role in distinguishing different domains, this paper proposes a low-dimension KGE model, named dual Archimedean spirals knowledge graph embedding model (DuASE). DuASE maps entities with the same relation on the same Archimedean spiral. Different spirals can model various relations for domain distinguishing through parameter b, and different rotation angles (parameter θ) of the same spiral can model differ-

ent entities. Meanwhile, we propose the dual spiral regularizer to cluster the spirals into their respective domain space. The experimental results fully illustrate that DuASE can better model multi-domain KG than previous methods and avoid embedding overlapping. In addition, we construct the datasets n-MDKG for multi-domain KGE.

Limitations

In this study, we for the first time explore the extraction of domain-specific knowledge from knowledge graphs for KGE tasks. We believe that future work should address the complexity of integrating multifaceted domain knowledge and scaling the extraction process to accommodate the ever-expanding scope of knowledge graphs. Moreover, similar to the majority of KGE models, DuASE is unable to process new entities that are not present in the training data.

Ethical Considerations

The datasets used in this study are sourced from publicly available internet data, strictly adhering to legality and ethical principles. All data are anonymized and do not contain any personal identity information or sensitive data. We have followed principles of privacy protection and data security throughout the process of data collection and utilization. To ensure the legitimacy and appropriateness of data sourcing and usage, we exclusively utilized publicly released data, such as online databases, websites, social media, among others. In this study, we have conducted thorough data processing and desensitization to safeguard against any potential personal privacy implications.

Acknowledgments

We would like to extend our sincere thanks to all reviewers for their insightful comments and valuable suggestions. The work by Jiang Li was funded by the Research and Innovation Projects for Graduate Students in Inner Mongolia Autonomous Region. This work was funded by National Natural Science Foundation of China (Grant No. 62366036), National Education Science Planning Project (Grant No. BIX230343), Key R&D and Achievement Transformation Program of Inner Mongolia Autonomous Region (Grant No. 2022YFHH0077), The Central Government Fund for Promoting Local Scientific and Technological Development (Grant No. 2022ZY0198), Program for Young Talents of Science and Technology in Universities of Inner Mongolia Autonomous Region (Grant No. NJYT24033), Inner Mongolia Autonomous Region Science and Technology Planning Project (Grant No. 2023YFSH0017), Joint Fund of Scientific Research for the Public Hospitals of Inner Mongolia Academy of Medical Sciences (Grant No.2023GLLH0035), Inner Mongolia Autonomous Natural Science Foundation Project (Grant No. 2022QN06003).

References

Ivana Balazevic, Carl Allen, and Timothy M. Hospedales. 2019a. Multi-relational poincaré graph embeddings. In *Advances in Neural Information Processing Systems 32: Annual Conference on Neural Information Processing Systems 2019, NeurIPS 2019, December 8-14, 2019, Vancouver, BC, Canada*, pages 4465–4475.

Ivana Balazevic, Carl Allen, and Timothy M. Hospedales. 2019b. Tucker: Tensor factorization for knowledge graph completion. In *Proceedings of the 2019 Conference on Empirical Methods in Natural Language Processing and the 9th International Joint Conference on Natural Language Processing, EMNLP-IJCNLP 2019, Hong Kong, China, November 3-7, 2019*, pages 5184–5193. Association for Computational Linguistics.

Antoine Bordes, Nicolas Usunier, Alberto García-Durán, Jason Weston, and Oksana Yakhnenko. 2013. Translating embeddings for modeling multi-relational data. In *Advances in Neural Information Processing Systems 26: 27th Annual Conference on Neural Information Processing Systems 2013. Proceedings of a meeting held December 5-8, 2013, Lake Tahoe, Nevada, United States*, pages 2787–2795.

Ines Chami, Adva Wolf, Da-Cheng Juan, Frederic Sala, Sujith Ravi, and Christopher Ré. 2020. Low-dimensional hyperbolic knowledge graph embeddings. In *Proceedings of the 58th Annual Meeting of the Association for Computational Linguistics, ACL 2020, Online, July 5-10, 2020*, pages 6901–6914. Association for Computational Linguistics.

Linlin Chao, Jianshan He, Taifeng Wang, and Wei Chu. 2021. PairRE: Knowledge graph embeddings via paired relation vectors. In *Proceedings of the 59th Annual Meeting of the Association for Computational Linguistics and the 11th International Joint Conference on Natural Language Processing (Volume 1: Long Papers)*, pages 4360–4369, Online. Association for Computational Linguistics.

Tim Dettmers, Pasquale Minervini, Pontus Stenetorp, and Sebastian Riedel. 2018. Convolutional 2d knowledge graph embeddings. In *Proceedings of the Thirty-Second AAAI Conference on Artificial Intelligence,*

(AAAI-18), the 30th innovative Applications of Artificial Intelligence (IAAI-18), and the 8th AAAI Symposium on Educational Advances in Artificial Intelligence (EAAI-18), New Orleans, Louisiana, USA, February 2-7, 2018, pages 1811–1818. AAAI Press.

Manas Gaur, Kalpa Gunaratna, Vijay Srinivasan, and Hongxia Jin. 2022. ISEEQ: information seeking question generation using dynamic meta-information retrieval and knowledge graphs. In *Thirty-Sixth AAAI Conference on Artificial Intelligence, AAAI 2022, Thirty-Fourth Conference on Innovative Applications of Artificial Intelligence, IAAI 2022, The Twelveth Symposium on Educational Advances in Artificial Intelligence, EAAI 2022 Virtual Event, February 22 - March 1, 2022*, pages 10672–10680. AAAI Press.

Xiou Ge, Yun Cheng Wang, Bin Wang, and C-C Jay Kuo. 2023. Compounding geometric operations for knowledge graph completion. In *Proceedings of the 61st Annual Meeting of the Association for Computational Linguistics (Volume 1: Long Papers)*, pages 6947–6965.

Linmei Hu, Zeyi Liu, Ziwang Zhao, Lei Hou, Liqiang Nie, and Juanzi Li. 2023. A survey of knowledge enhanced pre-trained language models. *IEEE Transactions on Knowledge and Data Engineering*.

Guoliang Ji, Shizhu He, Liheng Xu, Kang Liu, and Jun Zhao. 2015. Knowledge graph embedding via dynamic mapping matrix. In *Proceedings of the 53rd Annual Meeting of the Association for Computational Linguistics and the 7th International Joint Conference on Natural Language Processing of the Asian Federation of Natural Language Processing, ACL 2015, July 26-31, 2015, Beijing, China, Volume 1: Long Papers*, pages 687–696. The Association for Computer Linguistics.

Diederik P. Kingma and Jimmy Ba. 2015. Adam: A method for stochastic optimization. In *3rd International Conference on Learning Representations, ICLR 2015, San Diego, CA, USA, May 7-9, 2015, Conference Track Proceedings*.

Timothée Lacroix, Nicolas Usunier, and Guillaume Obozinski. 2018. Canonical tensor decomposition for knowledge base completion. In *Proceedings of the 35th International Conference on Machine Learning, ICML 2018, Stockholmsmässan, Stockholm, Sweden, July 10-15, 2018*, volume 80 of *Proceedings of Machine Learning Research*, pages 2869–2878. PMLR.

Jiang Li, Xiangdong Su, and Guanglai Gao. 2023. Teast: Temporal knowledge graph embedding via archimedean spiral timeline. In *Proceedings of the 61st Annual Meeting of the Association for Computational Linguistics (Volume 1: Long Papers)*, pages 15460–15474.

Yankai Lin, Zhiyuan Liu, Maosong Sun, Yang Liu, and Xuan Zhu. 2015. Learning entity and relation embeddings for knowledge graph completion. In *Proceedings of the Twenty-Ninth AAAI Conference on Artificial Intelligence, January 25-30, 2015, Austin, Texas, USA*, pages 2181–2187. AAAI Press.

George A. Miller. 1995. Wordnet: A lexical database for english. *Commun. ACM*, 38(11):39–41.

Mojtaba Nayyeri, Bo Xiong, Majid Mohammadi, Mst. Mahfuja Akter, Mirza Mohtashim Alam, Jens Lehmann, and Steffen Staab. 2023. Knowledge graph embeddings using neural ito process: From multiple walks to stochastic trajectories. In *Findings of the Association for Computational Linguistics: ACL 2023, Toronto, Canada, July 9-14, 2023*, pages 7165–7179. Association for Computational Linguistics.

Maximilian Nickel, Volker Tresp, and Hans-Peter Kriegel. 2011. A three-way model for collective learning on multi-relational data. In *Proceedings of the 28th International Conference on Machine Learning, ICML 2011, Bellevue, Washington, USA, June 28 - July 2, 2011*, pages 809–816. Omnipress.

Shirui Pan, Linhao Luo, Yufei Wang, Chen Chen, Jiapu Wang, and Xindong Wu. 2024. Unifying large language models and knowledge graphs: A roadmap. *IEEE Transactions on Knowledge and Data Engineering*.

Apoorv Saxena, Adrian Kochsiek, and Rainer Gemulla. 2022. Sequence-to-sequence knowledge graph completion and question answering. In *Proceedings of the 60th Annual Meeting of the Association for Computational Linguistics (Volume 1: Long Papers), ACL 2022, Dublin, Ireland, May 22-27, 2022*, pages 2814–2828. Association for Computational Linguistics.

Fabian M. Suchanek, Gjergji Kasneci, and Gerhard Weikum. 2007. Yago: a core of semantic knowledge. In *Proceedings of the 16th International Conference on World Wide Web, WWW 2007, Banff, Alberta, Canada, May 8-12, 2007*, pages 697–706. ACM.

Zhiqing Sun, Zhi-Hong Deng, Jian-Yun Nie, and Jian Tang. 2019. Rotate: Knowledge graph embedding by relational rotation in complex space. In *7th International Conference on Learning Representations, ICLR 2019, New Orleans, LA, USA, May 6-9, 2019*. OpenReview.net.

Kristina Toutanova and Danqi Chen. 2015. Observed versus latent features for knowledge base and text inference. In *Proceedings of the 3rd workshop on continuous vector space models and their compositionality*, pages 57–66.

Théo Trouillon, Johannes Welbl, Sebastian Riedel, Éric Gaussier, and Guillaume Bouchard. 2016. Complex embeddings for simple link prediction. In *Proceedings of the 33nd International Conference on Machine Learning, ICML 2016, New York City, NY, USA, June 19-24, 2016*, volume 48 of *JMLR Workshop and Conference Proceedings*, pages 2071–2080. JMLR.org.

Laurens Van der Maaten and Geoffrey Hinton. 2008. Visualizing data using t-sne. *Journal of machine learning research*, 9(11).

Kai Wang, Yu Liu, Dan Lin, and Michael Sheng. 2021a. Hyperbolic geometry is not necessary: Lightweight Euclidean-based models for low-dimensional knowledge graph embeddings. In *Findings of the Association for Computational Linguistics: EMNLP 2021*, pages 464–474, Punta Cana, Dominican Republic. Association for Computational Linguistics.

Kai Wang, Yu Liu, Qian Ma, and Quan Z. Sheng. 2021b. Mulde: Multi-teacher knowledge distillation for low-dimensional knowledge graph embeddings. In *WWW '21: The Web Conference 2021, Virtual Event / Ljubljana, Slovenia, April 19-23, 2021*, pages 1716–1726. ACM / IW3C2.

Zhen Wang, Jianwen Zhang, Jianlin Feng, and Zheng Chen. 2014. Knowledge graph embedding by translating on hyperplanes. In *Proceedings of the Twenty-Eighth AAAI Conference on Artificial Intelligence, July 27 -31, 2014, Québec City, Québec, Canada*, pages 1112–1119. AAAI Press.

Bishan Yang, Wen-tau Yih, Xiaodong He, Jianfeng Gao, and Li Deng. 2015. Embedding entities and relations for learning and inference in knowledge bases. In *3rd International Conference on Learning Representations, ICLR 2015, San Diego, CA, USA, May 7-9, 2015, Conference Track Proceedings*.

Yongqi Zhang, Quanming Yao, Wenyuan Dai, and Lei Chen. 2020. Autosf: Searching scoring functions for knowledge graph embedding. In *36th IEEE International Conference on Data Engineering, ICDE 2020, Dallas, TX, USA, April 20-24, 2020*, pages 433–444. IEEE.

Wayne Xin Zhao, Kun Zhou, Junyi Li, Tianyi Tang, Xiaolei Wang, Yupeng Hou, Yingqian Min, Beichen Zhang, Junjie Zhang, Zican Dong, et al. 2023. A survey of large language models. *arXiv preprint arXiv:2303.18223*.

Yushan Zhu, Wen Zhang, Mingyang Chen, Hui Chen, Xu Cheng, Wei Zhang, and Huajun Chen. 2022. Dualde: Dually distilling knowledge graph embedding for faster and cheaper reasoning. In *WSDM '22: The Fifteenth ACM International Conference on Web Search and Data Mining, Virtual Event / Tempe, AZ, USA, February 21 - 25, 2022*, pages 1516–1524. ACM.

A Embedding Overlapping Discussion

We conduct experiments on n-MDKG and compute the embedding overlapping cross domains via Jaccard index. Algorithm 1 illustrate the computation on 3-MDKG with 3 domains. We compute the Jaccard index on each pair domains and then calculate the average of Jaccard index. The formula is: $J(A,B) = \frac{|A \cap B|}{|A \cup B|}$, where A and B are the two sets, $|A \cap B|$ represents the size of the intersection, and $|A \cup B|$ represents the size of the union. It's important to note that Jaccard index is suitable for discrete entity embeddings and two entity embeddings are considered to be overlapping when their distance is smaller than a pre-defined very small threshold d.

Algorithm 1: Jaccard index

Input: A: domain A
B: domain B
C: domain C
$n_{a\cap b}$: the number of the overlapped entities in ($|A \cap B|$)
$n_{a\cap c}$: the number of the overlapped entities in ($|A \cap C|$)
$n_{b\cap c}$: the number of the overlapped entities in ($|B \cap C|$)
$n_{a\cup b}$: the number of entities in $A \cup B$
$n_{a\cup c}$: the number of entities in $A \cup C$
$n_{b\cup c}$: the number of entities in $B \cup C$

Output: Jaccard index=
$\frac{1}{3} \times (\frac{n_{a\cap b}}{n_{a\cup b}} + \frac{n_{a\cap c}}{n_{a\cup c}} + \frac{n_{b\cap c}}{n_{b\cup c}})$

We report the link prediction performance and Jaccard index of two representation models (TransE and RotatE) and the proposed DuASE in the case of different number of domains in the following Table 4. As the number of domains increases, the Jaccard index increases and embedding overlapping tends to be more obvious. We can see that DuASE makes domain constraints that mitigate the embedding overlap, leading to competitive results. This indicates that overlapping embeddings across different domains impair the effectiveness of link prediction.

	MRR	H@1	H@10	Jaccard index
TransE(3-MDKG)	0.126	0.082	0.214	0.282
TransE(6-MDKG)	0.170	0.098	0.310	0.371
TransE(9-MDKG)	0.029	0.014	0.057	0.404
RotatE(3-MDKG)	0.202	0.120	0.369	0.246
RotatE(6-MDKG)	0.230	0.172	0.338	0.302
RotatE(9-MDKG)	0.212	0.161	0.309	0.325
DuASE(3-MDKG)	0.301	0.211	0.475	0.221
DuASE(6-MDKG)	0.287	0.236	0.382	0.287
DuASE(9-MDKG)	0.324	0.278	0.340	0.299

Table 4: The result of Jaccard index on n-MDKG

B Modeling Key Relation Patterns

In addition, several important relation patterns have been extensively studied in KGE models (Sun et al., 2019). Understanding and capturing these relation patterns are essential for developing accurate and effective KGE models including:

- **Symmetry** If $(e_1, r, e_2) \in \mathcal{T}, \forall e_1, e_2 \in \mathcal{E} \Rightarrow (e_2, r, e_1) \in \mathcal{T}$.
- **Antisymmetry** If $(e_1, r, e_2) \in \mathcal{T}, \forall e_1, e_2 \in \mathcal{E} \Rightarrow (e_2, r, e_1) \notin \mathcal{T}$.
- **Inversion** If $(e_1, r_1, e_2) \in \mathcal{T}, \forall e_1, e_2 \in \mathcal{E} \Rightarrow (e_2, r_2, e_1) \in \mathcal{T}$.
- **Composition** If $(e_1, r_1, e_2) \in \mathcal{T} \wedge (e_2, r_2, e_3) \in \mathcal{T}, \forall e_1, e_2, e_3 \in \mathcal{E} \Rightarrow (e_1, r_3, e_3) \in \mathcal{T}$.

We give some propositions and prove that DuASE can model important relation patterns, including symmetry, antisymmetry, inversion and composition.

Proposition 1. *DuASE can infer the symmetry relation pattern.*

Proof. If $(e_1, r, e_2) \in \mathcal{T}, (e_2, r, e_1) \in \mathcal{T}$, we have

$$\left.\begin{aligned} \mathbf{e_1} \circ S_h = \mathbf{e_2} \circ S_t \\ \mathbf{e_2} \circ S_h = \mathbf{e_1} \circ S_t \end{aligned}\right\} \Rightarrow S_h = -S_t. \tag{7}$$

Proposition 2. *DuASE can infer the antisymmetry relation pattern.*

Proof. If $(e_1, r, e_2) \in \mathcal{T}, (e_2, r, e_1) \notin \mathcal{T}$, we have

$$\left.\begin{aligned} \mathbf{e_1} \circ S_h = \mathbf{e_2} \circ S_t \\ \mathbf{e_2} \circ S_h \neq \mathbf{e_1} \circ S_t \end{aligned}\right\} \Rightarrow S_h \neq -S_t. \tag{8}$$

Proposition 3. *DuASE can infer the inversion relation pattern.*

Proof. If $(e_1, r_1, e_2) \in \mathcal{T}, (e_2, r_2, e_1) \in \mathcal{T}$, we have

$$\left.\begin{aligned} \mathbf{e_1} \circ S_{h1} + \mathbf{r_1} = \mathbf{e_2} \circ S_{t1} \\ \mathbf{e_2} \circ S_{h2} + \mathbf{r_2} = \mathbf{e_1} \circ S_{t2} \end{aligned}\right\} \Rightarrow \\ (S_{h1} \circ S_{h2} = S_{t1} \circ S_{t2}) \wedge (\mathbf{r_1} = -\mathbf{r_2}). \tag{9}$$

Proposition 4. *DuASE can infer the composition relation pattern.*

Proof. If $(e_1, r_1, e_2) \in \mathcal{T}, (e_2, r_2, e_3) \in \mathcal{T}, (e_1, r_3, e_3) \in \mathcal{T}$, we have

$$\left.\begin{aligned} \mathbf{e_1} \circ S_{h1} + \mathbf{r_1} = \mathbf{e_2} \circ S_{t1} \\ \mathbf{e_2} \circ S_{h2} + \mathbf{r_2} = \mathbf{e_3} \circ S_{t2} \\ \mathbf{e_1} \circ S_{h3} + \mathbf{r_3} = \mathbf{e_3} \circ S_{t3} \end{aligned}\right\} \Rightarrow \\ (S_{h3} = S_{h1} \circ S_{h2}) \wedge (S_{t3} = S_{t1} \circ S_{t2}) \\ \wedge (\mathbf{r_3} = \mathbf{r_1} \circ S_{h2} + \mathbf{r_2} \circ S_{t1}). \tag{10}$$

C Relation with Other Distance-based KGE Models

DuASE is a general form of quite a few distance-based KGE models. That is, we can derive their scoring functions from that of DuASE by setting translation to certain forms. Four examples are given below

Derivation of TransE (Bordes et al., 2013) DuASE removed the spiral domain constraint and regarded S_h, S_t as the identity matrix I. In addition, DuASE needs to remove the entity embedding range constraints. Then, we get the scoring function of TransE as

$$\begin{aligned} f_r(\boldsymbol{e}_h, \boldsymbol{e}_t) &= - \parallel \boldsymbol{e}_h \circ S_h + \boldsymbol{e}_r - \boldsymbol{e}_t \circ S_t \parallel \\ &= - \parallel \boldsymbol{e}_h \circ I + \boldsymbol{e}_r - \boldsymbol{e}_t \circ I \parallel \\ &= - \parallel \boldsymbol{e}_h + \boldsymbol{e}_r - \boldsymbol{e}_t \parallel \end{aligned} \tag{11}$$

Derivation of RotatE (Sun et al., 2019) We can derive the scoring function of RotatE from DuASE by setting the $\boldsymbol{e_r}$ component to 0 and S_t component to I. In addition, DuASE needs to remove the entity embedding range constraints. Then, we get the scoring function of RotatE as

$$\begin{aligned} f_r(\boldsymbol{e}_h, \boldsymbol{e}_t) &= - \parallel \boldsymbol{e}_h \circ S_h + \boldsymbol{e}_r - \boldsymbol{e}_t \circ S_t \parallel \\ &= - \parallel \boldsymbol{e}_h \circ S_h - \boldsymbol{e}_t \parallel \end{aligned} \tag{12}$$

Derivation of CompoundE (Ge et al., 2023) We can derive the scoring function of CompoundE from DuASE by adding extra translation component T, rotation component R and setting $\boldsymbol{e}_r$ component to 0. In addition, DuASE needs to remove the entity embedding range constraints. Then, we get the scoring function of CompoundE as

$$\begin{aligned} f_r(\boldsymbol{e}_h, \boldsymbol{e}_t) &= - \parallel \boldsymbol{e}_h \circ S_h + \boldsymbol{e}_r - \boldsymbol{e}_t \circ S_t \parallel \\ &= - \parallel \boldsymbol{e}_h \circ S_h \circ T \circ R - \\ &\quad \boldsymbol{e}_t \circ S_t \circ T \circ R \parallel \end{aligned} \tag{13}$$

Although the score function of DuASE can be derived to other models, there is an essential difference in the geometric significance of the models. Our model uses spirals to model the multi-domain KG. To better model the multi-domain KGs and facilitate the link prediction performance, the KGE methods should equip two abilities. The first one is to model different relations so as to distinguish the knowledge triplets from different domains. The second one is to distinguish the entities within the same domain. According to our analysis, we found that spirals can fulfill these two requirements. Different spirals can model various domains through the types of relations (parameter b), and the rotation angle of the spiral (parameter θ) can model different entities on the same spiral.

D Statistics of n-MDKG

Table 5 shows the details of our proposed multi-domain KGE dataset. $|\mathcal{E}|$ and $|\mathcal{R}|$ represent the sets of entities and relations, respectively. The domain information of these three datasets are as follows:

- **3-MDKG** dataset covers 3 domains including education, film and sports.
- **6-MDKG** dataset covers 6 domains including medicine, education, film, sports, politics and dictionary.
- **9-MDKG** dataset covers 9 domains including medicine, education, film, sports, politics, dictionary, geography, automotive and modern stars.

Dataset	$\lvert\mathcal{E}\rvert$	$\lvert\mathcal{R}\rvert$	#Train	#Valid	#Test
3-MDKG	8,691	69	90,130	918	922
6-MDKG	90,275	361	429,810	4,383	4,391
9-MDKG	102,880	426	456,281	5,200	5,211

Table 5: Statistics of the 3-MDKG, 6-MDKG and 9-MDKG.

E Statistics of the Benchmark Datasets

WN18RR is a benchmark dataset for link prediction in the WordNet (Miller, 1995) knowledge graph. FB15K-237 is a variant of the Freebase knowledge graph. YAGO3-10 is a large-scale subset of the YAGO knowledge graph. The domain information of these three datasets is not described and investigated in previous works. Table 6 shows the details of the statistics of the benchmark datasets.

Dataset	$\lvert\mathcal{E}\rvert$	$\lvert\mathcal{R}\rvert$	#Train	#Valid	#Test
WN18RR	40,943	11	86,853	3034	3134
FB15K-237	14,541	237	272,115	17,535	20,466
YAGO3-10	123,182	37	1,079,040	5,000	5,000

Table 6: Statistics of the WN18RR, FB15K-237 and YAGO3-10.